THE ASTROPHYSICAL JOURNAL, 187:271–274, 1974 January 15

THE ORIENTATION OF MAGNETIC AXES IN Ap STARS: AN ALTERNATIVE INTERPRETATION OF THE COMPONENT WITH SMALL OBLIQUITY

ERMANNO F. BORRA
Hale Observatories, Carnegie Institution of Washington, California Institute of Technology
Received 1973 July 12; revised 1973 August 24

ABSTRACT

Zeeman-analyzed line profiles have been computed for oblique-rotator models and decentered-dipole configurations of the magnetic-field geometry. It is argued on the basis of these profiles that periodic magnetic variables with nonreversing magnetic fields can be interpreted as having the magnetic axis nearly orthogonal to the rotation axis. These objects have been previously interpreted as having the magnetic and rotational axes nearly aligned.

Subject headings: magnetic stars — peculiar A stars — Zeeman effect

I. INTRODUCTION

Preston (1967) has made a statistical investigation of the orientation of the magnetic axes in the known periodic magnetic variables. He defines $r = H_e(\text{min})/H_e(\text{max})$ as the ratio of the minimum to maximum longitudinal field of the magnetic curve. Assuming that the rotation axes are randomly oriented in the sky, he computes for a given β (the angle between magnetic and rotation axes) the probability $P_\beta(r)dr$ that a star will have an observed value of r between r and $r + dr$. Preston found that the observed distribution of r in the then known magnetic variables was consistent with a large value of β in all of those stars. In view of the later addition of several more periodic variables with $r > 0$, Preston (1971) has modified those conclusions to admit a component of small β.

Landstreet (1970) has proposed a decentered-dipole model for the geometry of the magnetic field of the Ap stars. This model is attractive as it can explain many hitherto unexplained features of the Ap stars (Preston 1971). Landstreet finds that the distributions of $P_\beta(r)$ using this model differ in detail from the centered dipole case but do not modify Preston's conclusions of a 50-50 admixture of stars with large and small β. The theoretical implications of the obliquity problem for the internal dynamics of the oblique-rotator model have been considered by Mestel and Takhar (1972).

In this work it is argued, on the basis of theoretical Zeeman-analyzed line profiles, that the decentered-dipole model can greatly modify Preston's conclusions. The excess of stars with $r > 0$ could be interpreted as the contribution of objects with large β and large decentering parameter.

II. COMPUTATIONS

In the following, we will consider only the oblique-rotator model. We will examine decentered-dipole models with $\beta = 90°$ to see whether it is possible to reconcile the observed distribution of r with a unique, large value of the obliquity for all the magnetic variables.

The computer program has been briefly described by Borra (1973) and in greater detail by Borra (1972). The wavelength dependence of the absorption coefficients is taken to be Gaussian, the saturated line is assumed to have a simple triplet Zeeman pattern, a wavelength $\lambda = 4260$ Å, and a Landé g-factor $g = 1.2$.

Figure 1 shows theoretical Zeeman-analyzed line profiles at selected parts of the cycle for a model with the rotational axis inclined at an angle $i = 90°$ to the line of sight. The equatorial velocity is $v_e = 0.0$ km s^{-1}.

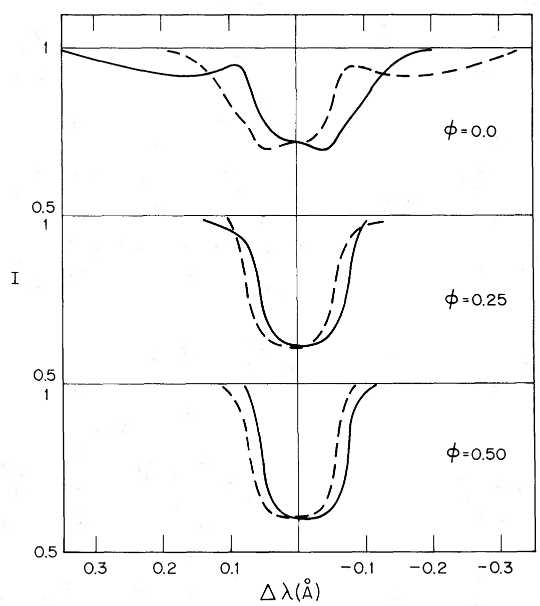

FIG. 1.—Left and right circular polarized components at three parts of the cycle for the model with H_p = 30,000 gauss and a = 0.5.

The parameter that defines the displacement of the dipole center from the center of the star, along the dipole's axis of symmetry, is $a = 0.5$ (stellar radius units). The local field of the strongest pole is $H_p = 30{,}000$ gauss. From here on, phase $\phi = 0.0$ of the models is taken to be when the line of sight lies in the plane defined by the axis of rotation and dipole axis, the observer viewing the strongest pole.

It is immediately apparent from figure 1 that if we measure the Zeeman displacements, using all but the far wings of the lines, we do not see a reversal of the sign of the longitudinal field. It is most unlikely that a photographic observer would see the extended wings at $\phi = 0.0$, because of their weakness compared with the rest of the line and grain noise and because of blends with neighboring lines.

The effect we see in figure 1 is caused by the geometry of the magnetic field. At $\phi = 0.0$ the visible disk has regions (at the disk center) of strong local surface field (H_s^l) whose longitudinal component (H_e^l) has the opposite sign than H_e^l of surrounding regions of smaller H_s^l. For the model considered and phase 0.0, $H_s^l = H_p = 30{,}000$ gauss at the center of the disk and $H_s^l < 3000$ gauss near the limb. The regions of

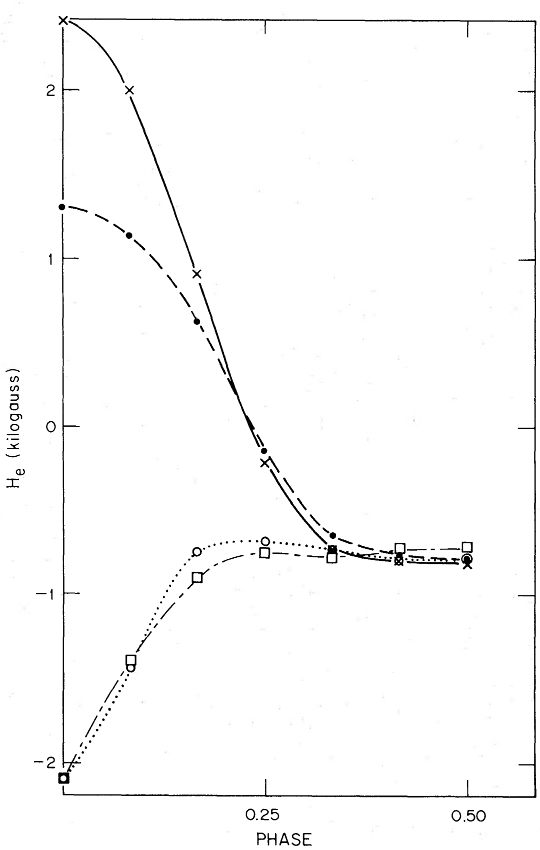

FIG. 2.—For half of the cycle of the model of fig. 1 we have plotted: H_e (*filled circles*); H_e^c (*crosses*); H_{e7} (*open circles*); H_{e3} (*open squares*). See text for more details.

weak field, which cover most of the disk, contribute to the core of the lines. The regions of strong field contribute to the far wings because of the large Zeeman separation of their σ components. The reversal of polarity (from $\phi = 0.5$) is carried by the regions of strong H_s^l and appears thus in the far wings.

In figure 2 we have, throughout half the cycle, plotted values of H_e obtained in different conditions:

$$H_e = \frac{\int H_e^l I \, dA}{\int I \, dA}\,, \tag{1}$$

where I is the local surface brightness of each area element dA;

$$H_e^c = \Delta\lambda / 9.33 g \lambda^2 \tag{2}$$

with

$$\Delta\lambda = \frac{\int \lambda r_L(\lambda) d\lambda}{\int r_L(\lambda) d\lambda} - \frac{\int \lambda r_R(\lambda) d\lambda}{\int r_R(\lambda) d\lambda}\,, \tag{3}$$

where $r_L(\lambda)$ and $r_R(\lambda)$ are the depression profiles of the Zeeman-analyzed components. We will obtain two more values of the longitudinal field (H_{e3} and H_{e7}) from equation (2) to illustrate the effect on the Zeeman displacements when different parts of the line are used in determining $\Delta\lambda$. It is difficult to reproduce numerically the actual weight that the eye gives to different parts of the profiles in determining the effective wavelengths of the Zeeman-analyzed components. There is probably a tendency to emphasize the core of the lines. First the Zeeman-analyzed profiles are convolved with a Gaussian instrumental profile of 0.07 Å half-width. A photographic characteristic curve is then applied to the profiles for an optimum photographic exposure (density 1.0 at the continuum). We thus obtain transmission profiles that are then normalized to 0.0 at the continuum and 1.0 at maximum transmission. Only the part of the transmission profiles greater than 0.7 (30% from the point of highest transmission) is used in computing $\Delta\lambda$ from equation (3) to get H_{e3}; only the part greater than 0.3 (70% from the point of highest transmission) to obtain H_{e7}. We can see from figure 2 that, although close to $\phi = 0.0$, H_e^c does not reproduce H_e well, it does show a reversal of polarity which neither H_{e7} nor H_{e3} indicates.

A feature of figures 1 and 2 which appears surprising at first is that the core of the line indicates a more negative field when the observer views the positive pole (phase 0.0). Figure 3 shows a section of the star along the axis of symmetry of the dipole. The two orthogonal components of the magnetic-field vector lying in this plane are drawn as arrows with a length proportional to the value of the components. At phase 0.0 the observer views the strongest pole (positive polarity). However, we can see that only regions near the center of the visible disk have a positive longitudinal component (arrows pointing toward the observer). For

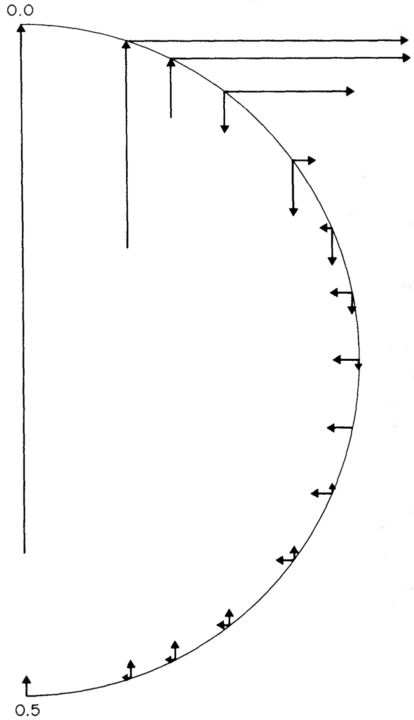

FIG. 3.—The section of the model with $a = 0.5$, taken along the axis of symmetry of the dipole, shows the orthogonal components of the magnetic field lying in this plane. The length of the arrows is proportional to the value of the components. The position of the observer at phases 0.0 and 0.5 is indicated on the figure.

regions nearer the limb the longitudinal component is negative. These regions of negative polarity give most of the Zeeman displacement in the core. The regions of positive polarity do not do so, as explained earlier (remember that the separation of the σ components is proportional to the magnetic field strength and not to the longitudinal component only). If we compare the magnitude of the average longitudinal component of the regions of negative polarity seen at phase 0.0 with the average longitudinal component over the disk seen at phase 0.5, we can readily understand why we see a more negative field (in the core of the lines) at phase 0.0. This qualitative discussion holds only if rotation is unimportant.

The model illustrated in figures 1 and 2 is a rather striking illustration of the effect proposed. However, the following changes in the main parameters of the model decrease the effect: a decrease in a, an increase in v_e, a decrease in H_p. Because of the large number of possible combinations of those parameters, we will consider only changes (at $\phi = 0.0$) in one parameter, keeping the others equal to those of the model of figure 1. A model with $a = 0.2$ still shows a reversal of polarity near the center of the line; however, because of the large and more uniform surface field, the triplet pattern is resolved and the reversal in the wing is unambiguous. A model with $a = 0.4$ shows the effect with H_s small enough that the triplet is not clearly resolved. A value of $v_e = 15 \text{ km s}^{-1}$ totally destroys the effect, which is still clearly present at 10 km s^{-1}. At $H_p = 10{,}000$ gauss the effect is still present; further reduction of H_p will cancel the effect, although the splitting is so small as to be difficult to measure photographically.

As an illustration of an intermediate case, we have plotted in figure 4 H_e, H_e^c, H_{e3}, H_{e7} for a model with $H_p = 30{,}000$ gauss; $i = 30°$, $\beta = 90°$; $a = 0.3$; $v_e = 20 \text{ km s}^{-1}$. H_{e7} shows a small positive value at $\phi = 0.0$, while H_{e3} is negative throughout the whole cycle. The shapes of the H_{e3} and H_{e7} curves are very similar to the curves of magnetic variables with $r > 0$ with their broad minimum (or maximum) and sharp maximum (or minimum) of the longitudinal field. Note that both $|H_{e7}|$ and $|H_{e3}|$ overestimate the absolute value of H_e near $\phi = 0.5$. This is caused by

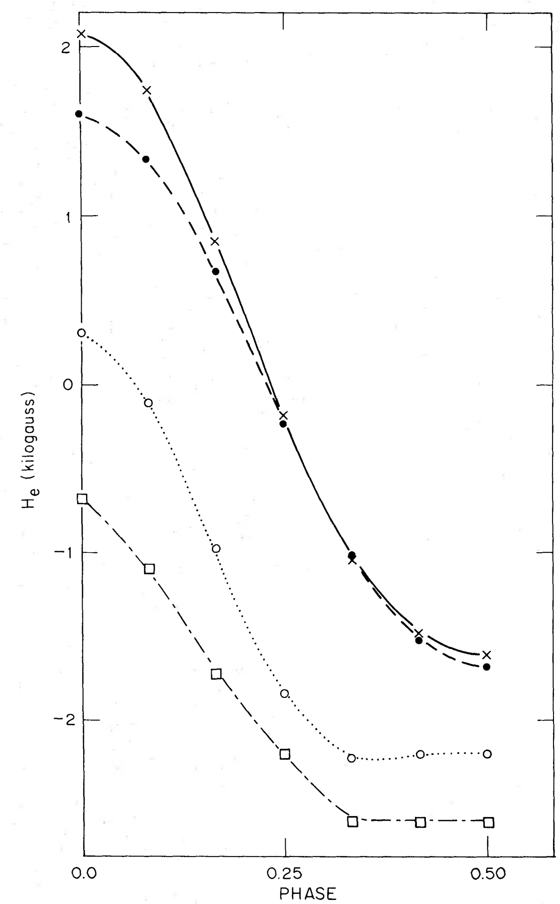

FIG. 4.—The model with $H_p = 30{,}000$ gauss and $a = 0.3$ is illustrated in this figure. Symbols used are the same as in fig. 2.

the shapes of the Zeeman-analyzed line profiles, which are in turn caused by a combination of field geometry and rotational Doppler shifts.

III. DISCUSSION

From the models illustrated, we see that it is possible to interpret the excess number of stars with $r > 0$ as stars with large β and large a.

An objection which could be raised is that the models can have large H_s (for $H_p = 30{,}000$ gauss and $a = 0.5$; $H_s = 9600$ gauss at $\phi = 0.0$, but $H_s = 1250$ gauss at $\phi = 0.5$). Preston (1971*b*) finds smaller values of H_s for some of the stars with $r > 0$. However, these values of H_s are based on the width of the lines as seen photographically. Figure 1 shows that the line profiles predicted have sharp cores (to obtain the unpolarized profiles, add the intensity of the components and divide by 2). The extended wings at $\phi = 0.0$ would not be seen, thus would appear to indicate a smaller value of H_s. Moreover, most of the values of H_s obtained by Preston are based only on one spectrogram. For decentered dipoles, H_s can vary greatly throughout the cycle.

If we examine the presently known periodic variables with $r > 0$ (HD 188041, HD 215441, 78 Vir, HD 24712, HD 111133, 52 Her), we see that all but 52 Her have $v \sin i \leq 10.0$ km s^{-1}. Consider that (Preston 1971*b*) the number of magnetic Ap stars with $0.0 \leqslant v \sin i \leqslant 10.0$ is smaller than the number of magnetic Ap stars with $10 > v \sin i \leqslant 30$. It would appear that stars with $r > 0$ are overrepresented among the slower rotators. (If we confine ourselves to known periodic magnetic variables only, we reach the same conclusion.) This is in agreement with the decrease of the effect proposed with increasing $v \sin i$. On the other hand, a large $v \sin i$ does not exclude the effect. What is important is the relative size of H_p, a, and $v \sin i$. It is, however, possible that selection effect which can explain the large number of periodic Ap stars with $r > 0$ among slow rotators are present. The errors in the measurements of longitudinal fields increase with $v \sin i$. This will make it more difficult to find a period when the range of the longitudinal field is small. Also, if, for some unknown physical reason, stars with $r > 0$ tend to have small longitudinal fields, we will not see them among fast rotators.

There are two observational tests we can do to show that H_e actually reverses sign in the models considered. Photoelectric measurements of the circular polarization in the wings of a line whose width is large compared to the Zeeman splitting caused by H_p (such as a Balmer line) will show a reversal of polarity. High-resolution polarization scans in an unblended spectral line will show a simple S-shaped wavelength dependence of the circular polarization at phase 0.5 and a double-S at phase 0.0. (To obtain the fractional circular polarization from fig. 1, divide the difference of intensity by the sum, for a given wavelength.)

If those observations will show a reversal of polarity in the stars with $r > 0$, then an inference we will be able to make is that the dipole can be decentered both in the directions of the north and the south poles, as we have examples of stars where the longitudinal field appears to be always positive, as well as cases where it is always negative. If, on the other hand, these new observations will show no reversal of polarity, we will be able to infer that very decentered dipoles are not frequent, at least among the slow rotators.

In this work we have used decentered dipole geometries. However, we can make a similar discussion for any geometry in which small and large values of $H_s{}^l$ coexist on the visible disk.

I wish to thank the Carnegie Institution of Washington for the award of a Carnegie Postdoctoral fellowship and Dr. R. F. Howard for the use of the computing facilities of the solar division.

REFERENCES

Borra, E. F. 1972, unpublished Ph.D. thesis, University of Western Ontario.
———. 1973, *Ap. J.*, **183**, 587.
Mestel, L., and Takhar, H. S. 1972, *M.N.R.A.S.*, **156**, 419.
Landstreet, J. D. 1970, *Ap. J.*, **159**, 1001.
Preston, G. W. 1967, *Ap. J.*, **150**, 547.
———. 1971*a*, *Pub. A.S.P.*, **83**, 571.
———. 1971*b*, *Ap. J.*, **164**, 309.